

# Synthesis of Novel Dual Target Inhibitors of CDK12 and PARP1 and Their Antitumor Activities in HER2-Positive Breast Cancers

Shanshan Lin, Qingna Jiang, Xiuwang Huang, Jianhua Xu, Lixian Wu,\* and Yang Liu\*

Cite This: *ACS Omega* 2023, 8, 25574–25581

Read Online

ACCESS |



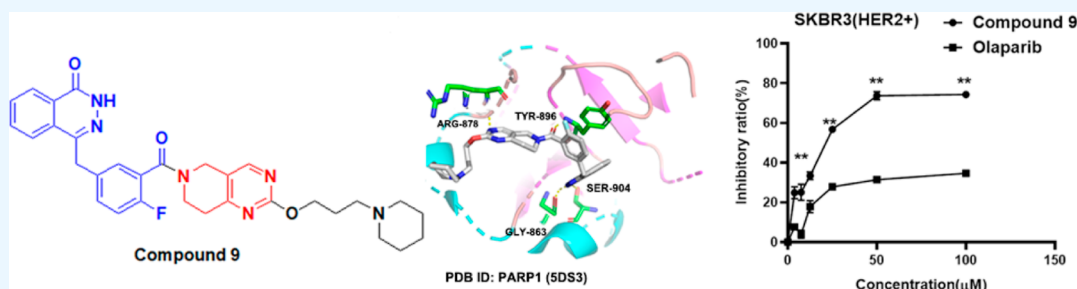
Metrics &amp; More



Article Recommendations



Supporting Information



**ABSTRACT:** Several anti-human epidermal growth factor receptor 2 (HER2) treatments have improved the landscape of HER2-positive breast cancer (BC) over the past few years; due to the heterogeneity of the disease itself, the drug resistance mechanisms and relapse are still the main issue in HER2-positive BC. Here, we intended to target simultaneous inhibition of both poly ADP-ribose polymerase 1 (PARP1) and cyclin-dependent kinase 12 (CDK12) that have had an impact on this disease up to their implementation in clinical practice. We successfully screened PARP1 inhibitors (PARPis) containing bicyclic tetrahydropyridine pyrimidines with antitumor activity. Most synthesized compounds with various alcohols were more effective at killing tumor cells than olaparib (ola), especially in HER2-positive cancer cells. Among them, compound 9 showed potent inhibitory effects on PARP1 enzymatic activity and the PAR protein level; moreover, the expression of CDK12 was inhibited by compound 9. Overall, compound 9 exhibited a significant antitumor effect by inhibiting DNA damage repair in tumors.

## 1. INTRODUCTION

Breast cancer (BC) remains one of the leading causes of morbidity and mortality in women to date.<sup>1</sup> Although BC can be detected at an early stage, some patients with HER2-positive BC are present or prone to developing regional or distant metastatic disease.<sup>2</sup> HER2 gene amplification and/or HER2 protein overexpression conferred aggressiveness in BC, leading to its poor prognosis.<sup>3,4</sup> The first-line treatment for HER2-positive BC patients is the dual-targeted therapy of pertuzumab and trastuzumab combined with taxanes; so far, up to 25% patients will relapse and have potential cardiotoxicity during the treatment. Therefore, we still urgently need other therapeutic drugs with novel mechanisms for the complex heterogeneity of HER2-positive BC. Interestingly, high expression of HER2 was accompanied by amplification of CDK12 in 71% of cases<sup>5,6</sup> and CDK12 has been suggested as a prospected druggable target in HER2-positive BC. CDK12 is a cyclin-dependent kinase that plays an important role in DNA damage repair (DDR) by influencing the expression of genes involved in homologous recombination (HR).<sup>7–9</sup> CDK12 inhibitors (CDK12is) decrease the expression of DDR-related genes to exert antitumor function, such as THZ531.<sup>10</sup> More interesting, plenty of studies have demonstrated that CDK12is exhibit synergistic effects with PARPis in HER2-positive BC

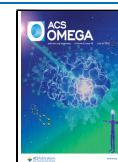
cells.<sup>11,12</sup> These suggested that we focus on the potential efficacy biomarkers of HER2-positive BC to select the best therapeutic strategy for each specific patient.

PARP1 is the most abundant enzyme in the PARP family that is involved in a wide scope of cellular processes. Suppression of PARP1 mainly leads to failure of base excision repair (BER) when single-strand DNA breaks (SSBs). Cells with loss of BER function were not chromosomal unstable<sup>13,14</sup> that cells still survive through HR. Based on the theory of synthetic lethal,<sup>15,16</sup> PARPis can only kill cancers that have lost HR function. Unfortunately, restoration of HR function, including the secondary mutation of BRCA, eventually resulted the emergence of resistance to PARPis.<sup>17,18</sup> We conjectured that restraining multiple HR genes together with PARP1, like CDK12, could play a synergistic antitumor in HER2-positive cancer cells. Tetrahydropyrido,<sup>43d</sup> pyrimidine exhibited cytotoxicity to tumor cells in a variety of tumor xenograft models, and

Received: May 15, 2023

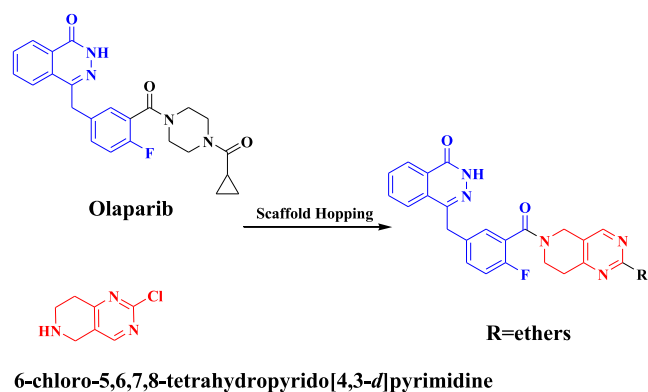
Accepted: June 23, 2023

Published: July 7, 2023



its mechanism of antitumor efficacy may point to multiple targets.<sup>19</sup> We designed a series of compounds that combined the core of ola with tetrahydropyrido,<sup>43d</sup> pyrimidine that with modified various amines, which have been proved dual-targeting inhibitors of PARP1 and EGFR.<sup>20</sup> To our surprise, multifarious ethers used to substitute with the 2-chloro atom on the pyrimidine ring of compound **1** also showed potent antitumor activity, especially in HER2-positive BC (Scheme 1).

### Scheme 1. Designed Route of Compounds 1–10



**1.1. Chemical Synthesis.** The products were prepared similarly to our previously published literature<sup>20,21</sup> Scheme 2. We used compound **1** to react with various alcohols under specific circumstances to produce final products (Scheme 2). Consistent with the previous published papers, the core of tetrahydropyrido,<sup>43d</sup> pyrimidine combined with 2-fluoro-5-[(1,2-dihydro-1-oxophthalazin-4-yl)methyl]benzoic acid on compound **9** still be further inserted to the active site of PARP1 (Figure 1A). As for the CDK12 docking model, key hydrogen bonds can be formed in compound **9** with GLN1015, ASP1016, and GLU1019 (Figure 1B). In conclusion, compound **9** has functions of modulating the activities of PARP1 and CDK12 by binding to the active site of PARP1 and CDK12.

## 2. RESULTS AND DISCUSSION

In this study, we first explored whether the CDK12 protein level was positively correlated with HER2 expression in BC. CDK12 protein was clearly promoted in HER2-positive SKBR3 than other HER2-negative BC (Figure 2A). All compounds were then used to execute the toxicity assessment against human cancer cell lines. Among them, compound **9**, which modified with piperidine ring with appropriate chain

length, showing a much greater potency against SKBR3 in a concentration-dependent manner compared with ola (Table 1 and Figure 2B,C). Compound **9** also retained a high sensitivity to BRCA mutant tumor strains than ola, including triple-negative BC HCC1937 (Table 1, Figure 2D,E). We attempted to discuss SAR from Table 1 with selective observations and claims supported by the data presented. Some compounds the carbon number between two heteroatoms is 3 in modified group whose activities are better than the carbon number 2 others in antitumor, like compounds **8** and **9**. Moreover, compounds with heteroatoms N greater than O in the modified group, such as compounds **2** and **4**. However, the above analysis needs to be further confirmed due to the limited data.

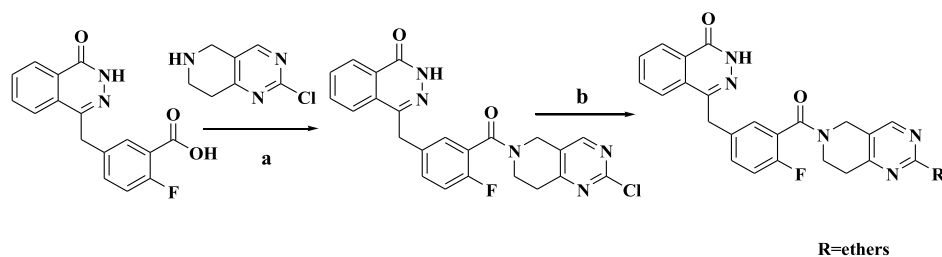
Next, we used an enzyme assay to investigate whether compound **9** could act on PARP1 and CDK12. The results showed that compound **9** had the similar inhibitory activity against PARP1 as ola, and the inhibitory rate of compound **9** was  $98.25\% \pm 4.46$  at  $0.1 \mu\text{M}$  (Figure 3A). We also found that compound **9** effectively inhibited the PARylation of PARP1 protein after treatment with azithromycin (ADM, a classic DNA damage drug) (Figure 3B,C). As expected, compound **9** also exhibited CDK12 inhibition activities comparable with those of ola in mRNA (Figure 3D) and protein level (Figure 3E,F). Because of the importance of CDK12 and PARP1 in DDR, we evaluated the effect of compound **9** on DDR. We inspected the production of  $\gamma\text{-H2AX}$  after administration of compound **9** was remarkably increased (Figure 4A,B).

## 3. CONCLUSIONS

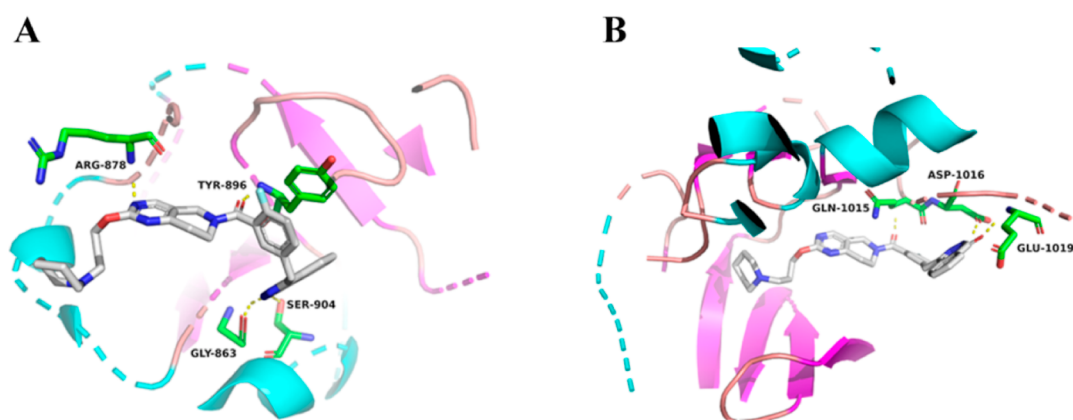
HER2 is one of the markers of aggressive BC, patients with HER2-positive tumor had inferior disease outcomes.<sup>22</sup> Although targeted therapies have had some success in HER2-positive BC, the drug resistance and poor prognosis still remain an important clinical concern and lead to relapse, metastasis, and death.<sup>23</sup> CDK12 was identified as one of the extra genes that conferred sensitivity to PARPis recently.<sup>24,25</sup> For example, a regimen of combining ola with the pan-CDK inhibitor dinaciclib could enhance the antitumor effect.

Our paper has proved the feasibility of combining PARP1 with other carcinogenic targets, including HSP90, EGFR, and CDK12. The structure of bicyclic tetrahydropyrido,<sup>43d</sup> pyrimidine targeted multiple proteins, and pethidine rings with a certain chain length in ether derivatives showed strong antitumor effects. Our work highlighted the synergistic effect of treatment that combined with PARP1 and CDK12 by increasing the amount of DNA damage, disrupting DNA repair, and thereby increasing the mortality of cancer cells.

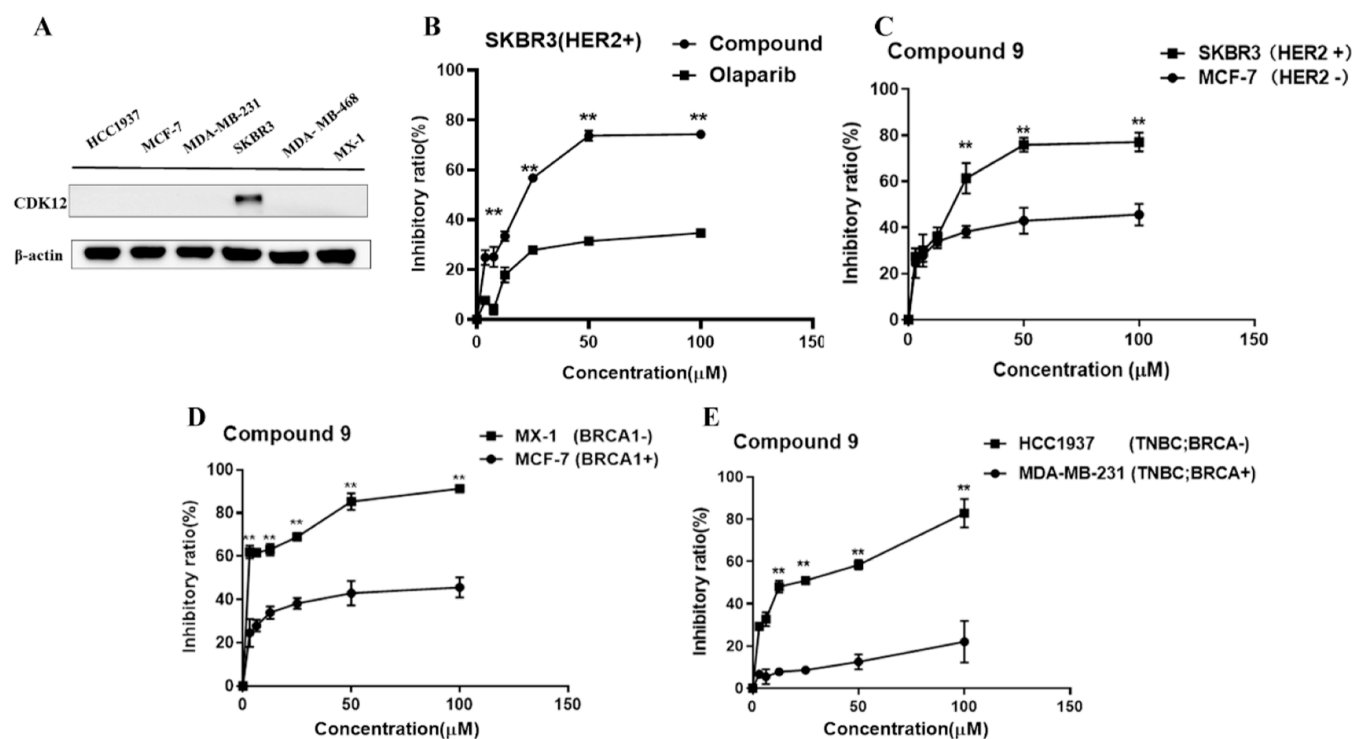
### Scheme 2. Synthesis Route for Compounds 1–10<sup>a</sup>



<sup>a</sup>(a) EDCl, HOBT, DIEA, DMF, RT, 24 h. (b) R, NaH, THF, RT, 10 h.



**Figure 1.** Software simulation of compound **9** docking with PARP1 (5DS3) or CDK12 (7NXJ). (A) The interaction of compound **9** binding to PARP1 (PDB ID: 5DS3). (B) The interaction of compound **9** binding to CDK12 (7NXJ). The carbon, nitrogen, and oxygen atoms of compound **9** are shown in white, blue, and red, and the residues in the PARP1 or CDK12 active site are shown in green, blue, and red. Hydrogen bonds are shown as yellow dashed lines.



**Figure 2.** (A) Evaluation of CDK12 protein expression in various BC. (B,C) The proliferation inhibition of compound **9** and ola in HER2-positive BC. (D,E) The proliferation inhibition of compound **9** in BRCA mutation BC. All the above results represent three independent experiments.  $**P < 0.01$ .

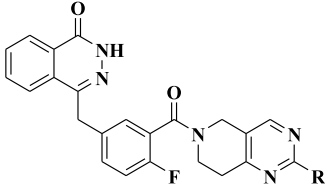
## 4. EXPERIMENTAL SECTION

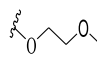
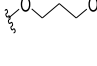
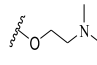
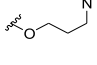
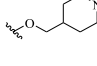
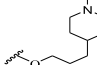
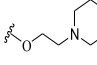
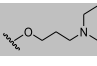
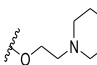
**4.1. General Information.** NMR spectra were recorded on a BRUKER BIOSPINNMR spectrometer (400 MHz). Chemical shifts are reported in parts per million (ppm) relative to internal standard residual solvent peaks (DMSO- $d_6 = 2.5$  ppm, methanol- $d_4 = 3.31$  ppm, chloroform- $d = 7.27$  ppm).  $^1\text{H}$  NMR coupling constants ( $J$ ) are reported in hertz (Hz), and multiplicity is indicated as follows: s (singlet), d (doublet), t (triplet), and m (multiplet). HRMS were obtained on an instrument named Agilent 7250& JEOL-JMS-T100LP Accu-TOF. Purities of the tested compounds determined by HPLC. Preparative HPLC was carried out on  $250 \times 10$  mm C-18 column using gradient conditions (50–100% B, flow rate = 1.0

mL/min, 10 min, detection at 245 nm). The eluents were as follows: solvent A ( $\text{H}_2\text{O}$ ) and solvent B ( $\text{CH}_3\text{OH}$ ).

**4.2. Docking Simulations.** PARP protein model (PDB ID: 5DS3) and ligand structures and CDK12 protein model (PDB ID: 7NXJ) and ligand structures followed standard preparation procedure using Auto Dock Tools 1.5.6. We used PYMOL 2.2.0. to perform all docking runs. The atoms of the compounds were colored, and the key residues in the active site of PARP1 and CDK12 protein were colored green, blue, and red, respectively. The hydrogen bonds were shown as yellow dot lines.

**4.3. General Procedure for Compounds 1–10.** **4.3.1.** 2-Chloro-5,6,7,8-tetrahydropyrido, $^{43d}$ pyrimidinyl)-[2-fluoro-5-[(4-oxo-3,4-dihydronaphthyridine)-1-yl)methyl]phenyl]-

Table 1. Chemical Structures and IC<sub>50</sub> Values (μM) of Synthesized Compounds in Cancer Cells


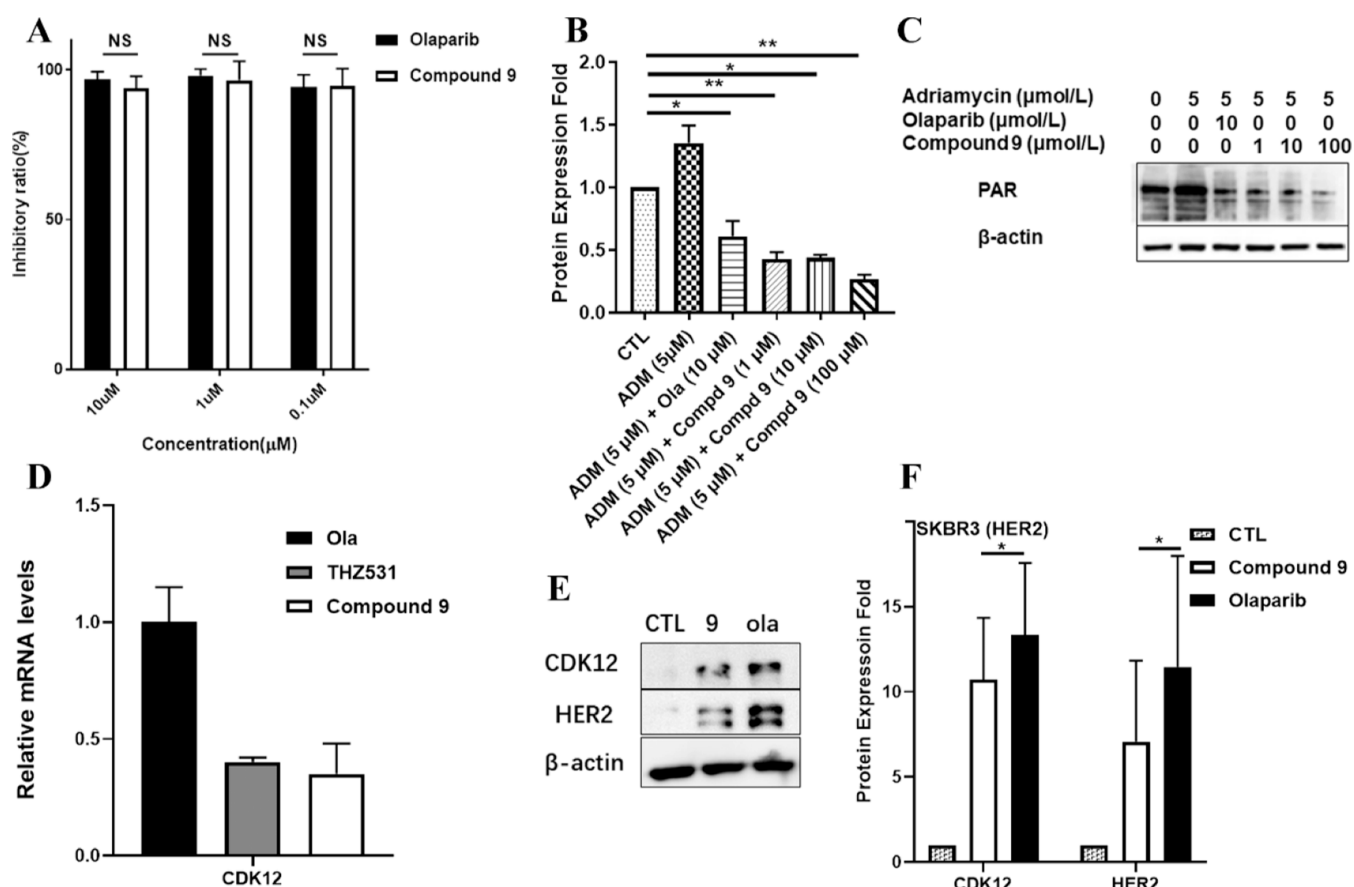
Compound	Substituents (R)	SKBR3 (BRCA <sup>wt</sup> , HER2 <sup>+</sup> )	MX-1 (BRCA1 <sup>-</sup> , HER2 <sup>-</sup> )	HCC1937 (BRCA1 <sup>-</sup> , HER2 <sup>-</sup> )	MCF-7 (BRCA <sup>wt</sup> , HER2 <sup>-</sup> )	MDA-MB-231 (BRCA <sup>wt</sup> , HER2 <sup>-</sup> )
1	Cl	> 200	> 200	> 200	> 200	> 200
2		113.5±4.34	34.9±7.19	185.8±8.9 2	ND	ND
3		100.4±3.39	26.5±1.11	63.3±2.19	ND	ND
4		94.9±1.45	12.9±2.24	30.6±7.23	ND	ND
5		63.6±3.32	126.4±3.3 5	24.1±2.21	ND	ND
6		74.6±2.60	17.6±1.90	25.3±2.54	ND	ND
7		> 200	26.02±2.6 7	91.2±3.28	ND	ND
8		> 200	> 200	99.0±3.22	ND	ND
9		20.23±1.44	1.6±1.34	18.6±5.41	>200	>200
10		> 200	21.4±5.76	> 200	ND	ND
Ola	--	232±5.50	35.8±8.89	> 200	>200	>200

**methanone Compound 1.** 2-Fluoro-5-[(4-oxo-3,4-dihydro-naphthyridin-1-yl)methyl]benzoic acid (50 mg, 0.15 mmol), EDCI (52 mg, 0.27 mmol) and HOBT (4 mg, 0.27 mmol) were dissolved in 5 mL of THF. After stirring at room temperature for 1 h, DIEA (1.88 mL, 13, 4 mmol) was added followed by 2-chloro-5,6,7,8-tetrahydropyrido,<sup>43d</sup>pyrimidine hydrochloride<sup>1</sup> (55 mg, 0.27 mmol) and the resulting solution was stirred under 25 °C 24 h. The reaction mixture with dichloromethane was washed three times with water. The material was placed on a silica gel column and eluted with PE/EA to give product. mp: 222.7–223.3 °C. <sup>1</sup>H NMR (400 MHz, chloroform-*d*): δ 11.85 (s, 1H), 8.51–8.40 (m, 1H), 8.39–8.03 (m, 1H), 7.80–7.72 (m, 2H), 7.49 (m, 1H), 7.42–7.31 (m, 2H), 7.06 (m, 1H), 4.72 (m, 2H), 4.40–4.20 (m, 2H), 4.15–3.51 (m, 2H), 3.18–2.77 (m, 2H). <sup>13</sup>C NMR (100 MHz, CDCl<sub>3</sub>): δ 166.11, 165.89, 165.36, 161.10, 159.30, 158.07, 157.52, 145.67, 143.46, 134.55, 134.52, 133.76, 132.13, 132.04, 129.62, 129.49, 129.30, 128.70, 128.10, 127.11, 124.94, 124.86, 123.28, 123.12, 120.39, 116.41, 116.19, 43.44, 40.88,

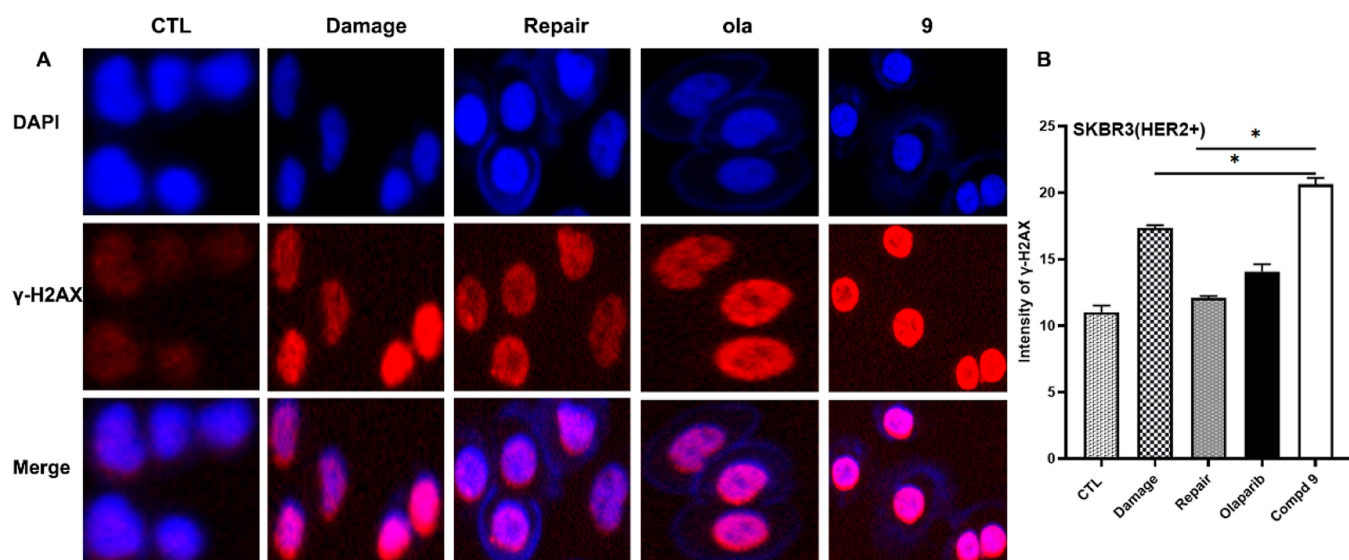
37.59, 31.95. HRMS (ESI<sup>+</sup>) *m/z*: [M + H] calcd for C<sub>23</sub>H<sub>17</sub>ClFN<sub>5</sub>O<sub>2</sub>, 448.11276; found, 450.11324.

**4.3.2. General Procedure for the Synthesis of the Target Compounds 2–10.** A solution of compound 1 (50 mg, 0.11 mmol), ether (0.33 mmol), and sodium hydrogen (13.32 mg, 0.56 mmol) was added to 10 mL of dry THF and allowed to react at room temperature for 10 h. The product was extracted with DCM (3 × 10 mL), the organic layer was dried over sodium sulfate, and the solvent was evaporated. The dry residue was purified by filtering through silica gel with petroleum ether/ethyl acetate (1:2) to give product.

**4.3.3. Analytical Data for Selected Final Compound 2.** mp: 187.2–187.7 °C. <sup>1</sup>H NMR (400 MHz, DMSO-*d*<sub>6</sub>): δ 12.60 (s, 1H), 8.51 (s, 1H), 8.45–8.03 (m, 1H), 8.18–7.59 (m, 3H), 7.64–7.07 (m, 3H), 4.77 (s, 2H), 4.40 (d, 2H), 4.34 (d, 2H), 4.01–3.45 (m, 4H), 3.29 (d, 3H), 3.07–2.29 (m, 2H). <sup>13</sup>C NMR (100 MHz, CDCl<sub>3</sub>): δ 165.78, 165.00, 163.89, 160.50, 157.10, 156.24, 145.50, 134.43, 133.70, 131.65, 129.52, 129.22, 128.33, 127.22, 124.99, 123.80, 123.62, 119.62, 116.40, 70.60, 66.62, 59.12, 41.00, 37.69, 32.11, 31.24. HRMS (ESI<sup>+</sup>)



**Figure 3.** (A) Enzyme kit (Trevigen, cat#: 4677-096-K) was used to determine the effects of compound 9 on PARP1 activity. (B,C) SKBR3 cells were treated with compound 9 or ola at 10 μM for 48 h after ADM treatment. (B) Quantification of (C). (D–F) Inhibitory effect of compound 9 on CDK12 activity. (D) SKBR3 cells were treated with ola, THZ531, and compound 9 at 10 μM for 48 h. (E,F) SKBR3 cells were treated with compound 9 or ola at 10 μM for 48 h. (F) Quantification of (E). All the above results represent three independent experiments. \**P* < 0.05, \*\**P* < 0.01.



**Figure 4.** Effect of compound 9 on DDR. (A) SKBR3 cells were treated with compound 9 or ola at 10 μM for 48 h after ADM treatment. High-content imaging (20×) was used to detect γ-H2AX levels. (B) Quantification of (A). (*n* = 49 fields, > 5000 cells counted per condition). All the above results represent three independent experiments. \**P* < 0.05.

*m/z*: [M + H]<sup>+</sup> calcd for C<sub>26</sub>H<sub>24</sub>FN<sub>5</sub>O<sub>4</sub>, 490.18851; found, 490.18911.

**4.3.4. Analytical Data for Selected Final Compound 3.**  
 mp: 159.0–160.7 °C. <sup>1</sup>H NMR (400 MHz, DMSO-*d*<sub>6</sub>): δ 12.60 (d, 1H), 8.75–8.12 (m, 2H), 7.98 (m, 1H), 7.94–7.79

(m, 2H), 7.79–7.58 (m, 2H), 7.42 (m, 1H), 4.58 (m, 2H), 4.32 (m, 4H), 4.09–3.73 (m, 2H), 3.65–3.40 (m, 4H), 3.24 (s, 2H), 2.95–2.45 (m, 3H). HRMS (ESI<sup>+</sup>) *m/z*: [M + Na] calcd for C<sub>27</sub>H<sub>26</sub>FN<sub>5</sub>O<sub>4</sub>, 526.18610; found, 526.18613.

**4.3.5. Analytical Data for Selected Final Compound 4.** mp: 226.8–229.3 °C. <sup>1</sup>H NMR (400 MHz, methanol-*d*<sub>4</sub>): δ 8.64–8.45 (m, 1H), 8.44–8.19 (m, 2H), 8.02–7.78 (m, 3H), 7.54 (m, 1H), 7.43 (m, 1H), 7.27–7.14 (m, 1H), 4.93 (s, 2H), 4.78–4.51 (m, 2H), 4.41 (d, 2H), 4.38–3.83 (m, 2H), 3.81–3.35 (m, 2H), 3.31–2.97 (m, 2H), 2.92 (d, 3H), 2.68 (s, 3H). <sup>13</sup>C NMR (100 MHz, CDCl<sub>3</sub>): δ 165.99, 165.22, 163.70, 160.84, 158.47, 157.12, 156.01, 145.46, 134.50, 133.63, 131.82, 131.57, 129.51, 128.26, 127.12, 124.96, 123.54, 119.62, 116.40, 65.06, 57.48, 45.46, 43.71, 40.97, 39.18, 37.67, 32.06, 31.21. HRMS (ESI<sup>+</sup>) *m/z*: [M + H] calcd for C<sub>27</sub>H<sub>27</sub>FN<sub>6</sub>O<sub>3</sub>, 503.22014; found, 503.22061.

**4.3.6. Analytical Data for Selected Final Compound 5.** mp: 227.0–230.5 °C. <sup>1</sup>H NMR (400 MHz, methanol-*d*<sub>4</sub>): δ 8.57 (d, 1H), 8.44–8.33 (m, 1H), 8.02–7.78 (m, 3H), 7.68–7.38 (m, 3H), 7.21 (m, 1H), 4.94–4.60 (d, 2H), 4.47–4.35 (m, 2H), 4.35–4.21 (m, 2H), 4.11 (s, 2H), 3.12–2.96 (m, 2H), 2.95–2.85 (m, 2H), 2.07–1.16 (m, 6H), 2.03–2.06 (m, 2H). <sup>13</sup>C NMR (100 MHz, CDCl<sub>3</sub>): δ 167.12, 166.17, 166.05, 165.89, 160.43, 159.48, 157.49, 156.59, 145.45, 134.51, 133.73, 131.71, 129.51, 128.33, 127.25, 125.19, 124.94, 123.36, 116.23, 45.18, 43.45, 40.89, 38.92, 37.64, 33.47, 31.99, 31.17, 24.95.

**4.3.7. Analytical Data for Selected Final Compound 6.** mp: 229.8–231.5 °C. <sup>1</sup>H NMR (400 MHz, methanol-*d*<sub>4</sub>): δ 8.52 (d, 1H), 8.40 (s, 1H), 8.22 (d, 1H), 8.00 (s, 1H), 7.92–7.82 (m, 2H), 7.52 (s, 1H), 7.43 (d, 1H), 7.19 (s, 1H), 4.94 (s, 2H), 4.86 (s, 2H), 4.60 (d, 1H), 4.49–4.41 (m, 2H), 4.25 (d, 2H), 3.69 (d, 1H), 3.67–3.35 (m, 2H), 3.29–2.95 (m, 2H), 2.95–2.58 (m, 3H), 1.55 (s, 2H), 0.92 (s, 1H). <sup>13</sup>C NMR (100 MHz, CDCl<sub>3</sub>): δ 165.62, 163.75, 162.65, 160.13, 159.48, 155.79, 154.82, 145.51, 134.19, 133.69, 131.63, 131.45, 129.54, 129.16, 128.39, 127.23, 125.04, 116.35, 112.83, 63.55, 46.68, 45.32, 44.13, 41.29, 39.67, 37.67, 32.33, 31.45, 25.53, 24.71. HRMS (ESI<sup>+</sup>) *m/z*: [M + H] calcd for C<sub>30</sub>H<sub>31</sub>FN<sub>6</sub>O<sub>3</sub>, 543.25144; found, 543.25182.

**4.3.8. Analytical Data for Selected Final Compound 7.** mp: 259.0–260.7 °C. <sup>1</sup>H NMR (400 MHz, DMSO-*d*<sub>6</sub>): δ 12.60 (s, 1H), 8.60 (d, 1H), 8.27 (d, 1H), 8.04–7.79 (m, 3H), 7.44 (d, 2H), 7.27 (m, 1H), 4.86 (s, 2H), 4.51 (s, 2H), 4.34 (d, *J* = 11.3 Hz, 2H), 4.11–3.82 (m, 2H), 3.53 (s, 2H), 3.18 (m, 2H), δ 3.10 (m, 2H), 2.95–2.58 (m, 3H), 2.00 (m, 2H), 1.98–1.80 (m, 2H), 1.64 (m, 2H), 1.39 (m, 2H), 1.31 (s, 1H). <sup>13</sup>C NMR (100 MHz, CDCl<sub>3</sub>): δ 167.11, 165.90, 165.20, 160.68, 159.44, 157.50, 156.04, 145.48, 134.57, 133.73, 132.10, 131.69, 129.51, 128.66, 128.29, 127.22, 124.93, 123.35, 116.22, 60.81, 60.42, 59.62, 45.19, 43.44, 40.89, 38.90, 37.59, 32.13, 31.99, 31.17, 29.83, 29.66. HRMS (ESI<sup>+</sup>) *m/z*: [M + H] calcd for C<sub>32</sub>H<sub>35</sub>FN<sub>6</sub>O<sub>3</sub>, 571.28011; found, 571.16240.

**4.3.9. Analytical Data for Selected Final Compound 8.** mp: 150.0–150.7 °C. <sup>1</sup>H NMR (400 MHz, chloroform-*d*): δ 11.68 (s, 1H), 8.55–8.39 (m, 1H), 8.32 (s, 1H), 7.85–7.64 (m, 3H), 7.36 (m, 2H), 7.06 (m, 1H), 5.31 (s, 2H), 4.83 (s, 2H), 4.57 (d, 2H), 4.30 (d, 2H), 3.74–3.47 (m, 2H), 2.97 (m, 3H), 2.86 (s, 1H), 2.72 (t, 4H), 1.61–1.03 (m, 4H). <sup>13</sup>C NMR (100 MHz, CDCl<sub>3</sub>): δ 176.56, 165.79, 165.04, 163.49, 160.84, 158.47, 157.19, 156.29, 145.49, 134.50, 133.65, 131.58, 129.50, 128.24, 127.12, 124.95, 123.51, 119.77, 116.19, 64.29, 56.68, 54.26, 43.71, 40.95, 37.66, 32.06, 24.80, 23.49, 22.55. HRMS

(ESI<sup>+</sup>) *m/z*: [M + H] calcd for C<sub>30</sub>H<sub>31</sub>FN<sub>6</sub>O<sub>3</sub>, 543.25108; found, 543.25144.

**4.3.10. Analytical Data for Selected Final Compound 9.** mp: 209.0–210.7 °C. <sup>1</sup>H NMR (400 MHz, DMSO-*d*<sub>6</sub>): δ 12.59 (s, 1H), 8.27 (d, 2H), 8.09–7.79 (m, 3H), 7.59–7.07 (m, 3H), 4.65 (s, 1H), 4.43–4.17 (m, 3H), 4.05 (s, 4H), 3.76–3.61 (m, 4H), 3.47 (t, 2H), 2.83–2.58 (m, 2H), 2.42–2.36 (m, 4H), 2.36–2.27 (m, 2H), 1.03 (t, 2H). <sup>13</sup>C NMR (100 MHz, CDCl<sub>3</sub>): δ 165.67, 165.21, 163.75, 162.69, 160.69, 160.54, 155.78, 154.84, 145.54, 134.26, 133.70, 131.62, 129.54, 129.12, 128.30, 127.19, 125.04, 124.00, 116.15, 63.12, 45.53, 44.22, 41.26, 39.62, 37.71, 36.16, 32.66, 32.33, 32.13, 31.45, 29.87. HRMS (ESI<sup>+</sup>) *m/z*: [M + H] calcd for C<sub>31</sub>H<sub>33</sub>FN<sub>6</sub>O<sub>3</sub>, 557.26678; found, 557.26709. Purity: 96.90%.

**4.3.11. Analytical Data for Selected Final Compound 10.** mp: 229.8–231.5 °C. <sup>1</sup>H NMR (400 MHz, chloroform-*d*): δ 11.62 (s, 1H), 8.60–8.39 (m, 1H), 8.20 (d, 1H), 7.75 (d, 3H), 7.37 (s, 2H), 7.16–6.98 (m, 1H), 4.84 (s, 1H), 4.46 (d, 3H), 4.31 (s, 2H), 3.72 (s, 4H), 3.17 (s, 2H), 2.92 (d, 2H), 2.82 (s, 2H), 2.59 (s, 4H). <sup>13</sup>C NMR (100 MHz, CDCl<sub>3</sub>): δ 166.01, 165.79, 165.02, 163.77, 160.75, 158.48, 157.12, 156.28, 145.52, 134.44, 133.68, 131.62, 129.52, 128.27, 127.17, 124.97, 123.74, 119.63, 116.40, 66.83, 66.78, 64.89, 57.50, 57.19, 53.91, 53.32, 43.74, 37.68, 32.11. HRMS (ESI<sup>+</sup>) *m/z*: [M + H] calcd for C<sub>29</sub>H<sub>29</sub>FN<sub>6</sub>O<sub>4</sub>, 545.23122; found, 545.23071.

**4.4. Biological Assays.** **4.4.1. MTT.** Human cancer cell lines were inoculated in a 96-well culture plate at a concentration of 180 μL per well. In the experimental group, 20 μL of different concentrations of the drug was added, and the control group was not added. Each group was set up with three parallel wells and cultured at 37 °C for 48 h. Added 5 μL/mL of MTT solution to 20 μL/well. After 4 h of incubation, the supernatant was removed, 150 μL of DMSO was added, the mixture was shaken for 10 min with a micro-oscillator, and the absorbance (OD value) at 570 nm was measured with a microplate reader. The cell growth inhibition rate was calculated according to the absorbance [cell growth inhibition rate = (control group OD – experiment group OD)/control group OD × 100%]. The IC<sub>50</sub> value was calculated by the Logit method, and the experiment was repeated three times and averaged.

**4.4.2. PARP1 Enzyme Assay.** The inhibition rate of the compound to the PARP1 enzyme was measured by using a commercially available universal PARP colorimetric assay kit (Trevigen, cat#: 4677-096-K). Reagents in the kit included PARP-HSA, 20× PARP Buffer, 10× PARP Cocktail, Histone-Coated Clear Strip wells, 200 mM 3-Aminobenzamide, 10× Strep-Diluent, Strep-HRP, 10× activated DNA. 50 μL per well 1× PARP buffer was added and allowed to stand for 30 min at room temperature. The plate was tapped on a paper towel and the 1× PARP buffer was discarded. 10 μL of PARP1 inhibitor (positive control drug Olaparib, each test compound) was added. 15 μL/hole PARP enzyme (0.5 Unit/15 μL) was added and allowed to stand for 10 min at room temperature. 25 μL portion per hole of 1× PARP Cocktail was added and placed at room temperature for 60 min. 200 μL/well of 1× PBS + 0.1% Triton X-100 was added and washed twice. 200 μL/well 1× PBS was added and washed twice. The plate was patted on a paper towel to ensure that the liquid is removed. 50 μL/well Strep-HRP was added and left at room temperature for 60 min. 200 μL/well 1× PBS+0.1% Triton X-100 was added and washed twice. Added 200 μL/well of 1× PBS and washed twice. Patted the plate on a paper towel to

ensure that the liquid is removed. Added 50  $\mu\text{L}$ /well Strep-HRP and left it at room temperature for 60 min. 200  $\mu\text{L}$ /well 1  $\times$  PBS + 0.1% Triton X-100 was added and washed twice. Added 200  $\mu\text{L}$ /well of 1 $\times$  PBS and washed twice. The plate was tapped on a paper towel to ensure the liquid is clear. Added 50  $\mu\text{L}$ /well 1 $\times$  Strep-Diluent, Strep-HRP, protected from light, and allowed to stand at room temperature for 15 min. The reaction was stopped by adding 50  $\mu\text{L}$ /well of 0.2 mol/L HCl. The microplate reader was tested at 450 nm. Inhibition rate (%) = (OD positive control – OD negative control – OD test compound well)/(OD positive control well – OD negative control)  $\times$  100%, and the inhibition rate of the test compound was obtained according to the OD value at different concentrations.

**4.4.3. Western Blot Analysis.** Placed the cell culture dish was placed on ice and the cells were washed with ice-cold PBS. The PBS was aspirated and then ice-cold lysis buffer. Scraped adherent cells were scraped off the dish using a cold plastic cell scraper and then gently transferred the cell suspension into a precooled microcentrifuge tube. Cells were trypsinized and washed with PBS prior to resuspension in lysis buffer in a microcentrifuge tube. Maintained constant agitation for 30 min at 4  $^{\circ}\text{C}$ . Centrifuged in a microcentrifuge at 4  $^{\circ}\text{C}$  for 20 min at 12,000 rpm. Gently removed the tubes from the centrifuge and placed them on ice, aspirated the supernatant and placed them in a fresh tube kept on ice, and discarded the pellet. Removed a small volume of lysate to perform a protein quantification assay. To reduce and denature samples, boiled each cell lysate in sample buffer at 98  $^{\circ}\text{C}$  for 5 min. Lysates can be aliquoted and stored at –20  $^{\circ}\text{C}$  for future use. Equal amounts of protein were loaded into the wells of the SDS-PAGE gel, along with molecular weight marker. 20–30  $\mu\text{g}$  of total protein were loaded from cell lysate. The gel was run for 1–2 h at 100 V. PVDF was activated with methanol for 1 min and rinsed with transfer buffer before preparing the stack. The membrane was blocked for 1 h at room temperature or overnight at 4  $^{\circ}\text{C}$  using blocking buffer. Incubated the membrane was incubated with appropriate dilutions of primary antibody overnight incubation at 4  $^{\circ}\text{C}$ . The membrane was washed three times with TBST, 5 min each. Incubated the membrane was incubated with the recommended dilution of conjugated secondary antibody in blocking buffer at room temperature for 1 h. Washed the membrane in three washes of TBST, 5 min each. Removed excess reagent was removed and the membrane was covered in transparent plastic wrap. Acquired images using darkroom development techniques for chemiluminescence.

**4.4.4. RT-PCR.** RNA was isolated using the Pure Link TM RNA kit (Invitrogen) and reverse transcribed using the cDNA Reverse Transcription Kit (Applied Biosystems) according to the manufacturer's guidelines. qPCR was performed using a Power SYBR Green PCR Master Mix (Applied Biosystems) in a Quant Studio 3 Real-Time PCR System (Applied Biosystems). Human CDK12 Forward Primer: CTAACAG-CAGAGAGCGTCACC; Reverse Primer: AAAGGTTTGA-TAACTGTGCCCA.

**4.4.5. High-Content Imaging Analysis.** SKBR3 cells were treated with the drug for 24 h. Collected cells were fixed, permeabilized, and refixed using a BD Fixation/Permeabilization Solution. Cells were incubated with r-H2AX quantification reagent (Abcam, ab81299) for 2 h at 37  $^{\circ}\text{C}$ . Cells were incubated with DAPI dye for nuclear staining for 30 min in the dark at room temperature, and quantitation was performed by

high content screen (Thermo Scientific Cellomics ArrayScan VTI).

**4.5. Animal Experiments.** All animal experiments were conducted in accordance with the animal experiment of this subject, were approved by the Experimental Animal Ethics Committee of Fujian Medical University (no. FJMU IACUC 2022-365) and carried out in accordance with ARRIVE (Animal Research: Reporting In Vivo Experiments Guidelines). Three healthy female SD rats fasted for 12 h before the experiment, and they were allowed to drink freely during the fasting period. The preprepared compound **9** solutions were given intravenously at a dose of 4 mg/kg (the formula was 4% DMSO + 30% PEG 300 + ddH<sub>2</sub>O). We fetched blood from the tail eyeball after injecting drug for 0.083, 0.167, 0.25, 0.5, 0.75, 1, 1.5, 2, and 4 h. Centrifuged at 3000 rpm and 4  $^{\circ}\text{C}$  for 10 min to separate the plasma, and data collection was performed on Lab Solutions LC/MS Ver. 5.5. The calculated plasma concentrations of compound **9** are expressed in ng/mL. The noncompartmental model of WinNonlin 5.2.1 was used to fit the blood drug concentration time of each rat to calculate the pharmacokinetic parameters.

## ■ ASSOCIATED CONTENT

### SI Supporting Information

The Supporting Information is available free of charge at <https://pubs.acs.org/doi/10.1021/acsomega.3c02912>.

Pharmacokinetic experiment data of compound **9**, general information, and HRMS/NMR spectra and HPLC data for all compounds (PDF)

## ■ AUTHOR INFORMATION

### Corresponding Authors

**Lixian Wu** – Department of Pharmacology, School of Pharmacy, Fujian Medical University (FMU), Fuzhou 350108, P. R. China; Fujian Key Laboratory of Natural Medicine Pharmacology, Fujian Medical University (FMU), Fuzhou 350108, PR China; [orcid.org/0000-0003-4689-6802](https://orcid.org/0000-0003-4689-6802); Email: [wlx-lisa@126.com](mailto:wlx-lisa@126.com)

**Yang Liu** – Fujian Key Laboratory of Natural Medicine Pharmacology and Department of Medicinal Chemistry, School of Pharmacy, Fujian Medical University (FMU), Fuzhou 350108, PR China; Email: [liuyang966@163.com](mailto:liuyang966@163.com)

### Authors

**Shanshan Lin** – Department of Pharmacy, The Second Affiliated Hospital of Fujian Medical University, Quanzhou 362046, P. R. China; Department of Pharmacology, School of Pharmacy, Fujian Medical University (FMU), Fuzhou 350108, P. R. China

**Qingna Jiang** – Department of Pharmacology, School of Pharmacy, Fujian Medical University (FMU), Fuzhou 350108, P. R. China

**Xiuwang Huang** – Department of Public Technology Service Center, Fujian Medical University (FMU), Fuzhou 350108, P. R. China

**Jianhua Xu** – Department of Pharmacology, School of Pharmacy, Fujian Medical University (FMU), Fuzhou 350108, P. R. China; [orcid.org/0000-0002-8990-6604](https://orcid.org/0000-0002-8990-6604)

Complete contact information is available at: <https://pubs.acs.org/doi/10.1021/acsomega.3c02912>

## Author Contributions

Y.L., L.W., and S.L. designed the research; L.W. and S.L. wrote the paper; S.L. performed the chemical synthesis studies; Q.J. and S.L. performed the biochemical and cellular studies; X.H. analyzed the results; and L.W., Y.L., and J.X. supervised the study.

## Notes

The authors declare no competing financial interest.

## ACKNOWLEDGMENTS

The authors gratefully acknowledge support of this project from the Natural Science Foundation of Fujian Province (2023J05151), National Natural Science Foundation of China (82073871), Startup Fund for Scientific Research, Fujian Medical University (2022QH1114), and the Doctor Nursery Foundation of the Second Affiliated Hospital of Fujian Medical University (BS202304). Thanks to the platform of the Public Technology Center of Fujian Medical University, the support of this project from AJE (<https://www.aje.cn/>) for English language editing and the School of Pharmacy Instrument Sharing Platform for providing technical support.

## REFERENCES

- (1) Sung, H.; Ferlay, J.; Siegel, R. L.; Laversanne, M.; Soerjomataram, I.; Jemal, A.; Bray, F. Global Cancer Statistics 2020: GLOBOCAN Estimates of Incidence and Mortality Worldwide for 36 Cancers in 185 Countries. *Ca-Cancer J. Clin.* **2021**, *71*, 209–249.
- (2) DeSantis, C. E.; Ma, J.; Gaudet, M. M.; Newman, L. A.; Miller, K. D.; Goding Sauer, A.; Jemal, A.; Siegel, R. L. Breast cancer statistics, 2019. *Ca-Cancer J. Clin.* **2019**, *69*, 438–451.
- (3) Bredin, P.; Walshe, J.; Denduluri, N. Systemic therapy for metastatic HER2-positive breast cancer. *Semin. Oncol.* **2020**, *47*, 259–269.
- (4) Chan, W.-L.; Lam, T.-C.; Lam, K.-O.; et al. Local and systemic treatment for HER2-positive breast cancer with brain metastases: a comprehensive review. *Ther. Adv. Med. Oncol.* **2020**, *12*, 1758835920953729.
- (5) Sircoulomb, F.; Bekhouche, I.; Finetti, P.; Adélaïde, J.; Hamida, A. B.; Bonansea, J.; Raynaud, S.; Innocenti, C.; Charafe-Jauffret, E.; Tarpin, C.; et al. Genome profiling of ERBB2-amplified breast cancers. *BMC Cancer* **2010**, *10*, 539.
- (6) Mertins, P.; Mani, D. R.; Ruggles, K. V.; Gillette, M. A.; Clauser, K. R.; Wang, P.; Wang, X.; Qiao, J. W.; Cao, S.; Petralia, F.; et al. Proteogenomics connects somatic mutations to signalling in breast cancer. *Nature* **2016**, *534*, 55–62.
- (7) Ekumi, K. M.; Paculova, H.; Lenasi, T.; Pospichalova, V.; Bösen, C. A.; Rybarikova, J.; Bryja, V.; Geyer, M.; Blazek, D.; Barboric, M. Ovarian carcinoma CDK12 mutations misregulate expression of DNA repair genes via deficient formation and function of the Cdk12/CycK complex. *Nucleic Acids Res.* **2015**, *43*, 2575–2589.
- (8) Blazek, D.; Kohoutek, J.; Bartholomeeusen, K.; Johansen, E.; Hulinkova, P.; Luo, Z.; Cimermanic, P.; Ule, J.; Peterlin, B. M. The Cyclin K/Cdk12 complex maintains genomic stability via regulation of expression of DNA damage response genes. *Genes Dev.* **2011**, *25*, 2158–2172.
- (9) Johnson, S. F.; Cruz, C.; Greifenberg, A. K.; Dust, S.; Stover, D. G.; Chi, D.; Primack, B.; Cao, S.; Bernhardt, A. J.; Coulson, R.; et al. CDK12 Inhibition Reverses De Novo and Acquired PARP Inhibitor Resistance in BRCA Wild-Type and Mutated Models of Triple-Negative Breast Cancer. *Cell Rep.* **2016**, *17*, 2367–2381.
- (10) Zhang, T.; Kwiatkowski, N.; Olson, C. M.; Dixon-Clarke, S. E.; Abraham, B. J.; Greifenberg, A. K.; Ficarro, S. B.; Elkins, J. M.; Liang, Y.; Hannett, N. M.; et al. Covalent targeting of remote cysteine residues to develop CDK12 and CDK13 inhibitors. *Nat. Chem. Biol.* **2016**, *12*, 876–884.
- (11) Joshi, P. M.; Sutor, S. L.; Huntoon, C. J.; Karnitz, L. M. Ovarian Cancer-associated Mutations Disable Catalytic Activity of CDK12, a Kinase That Promotes Homologous Recombination Repair and Resistance to Cisplatin and Poly(ADP-ribose) Polymerase Inhibitors. *J. Biol. Chem.* **2014**, *289*, 9247–9253.
- (12) Natrajan, R.; Wilkerson, P. M.; Marchiò, C.; Piscuoglio, S.; Ng, C. K.; Wai, P.; Lambros, M. B.; Samartzis, E. P.; Dedes, K. J.; Frankum, J.; et al. Characterization of the genomic features and expressed fusion genes in micropapillary carcinomas of the breast. *J. Pathol.* **2014**, *232*, 553–565.
- (13) Csizmar, C. M.; Saliba, A. N.; Swisher, E. M.; et al. PARP Inhibitors and Myeloid Neoplasms: A Double-Edged Sword. *Cancers* **2021**, *13*, 24.
- (14) Curtin, N. J.; Szabo, C. Poly(ADP-ribose) polymerase inhibition: past, present and future. *Nat. Rev. Drug Discovery* **2020**, *19* (10), 711–736.
- (15) Bryant, H. E.; Schultz, N.; Thomas, H. D.; Parker, K. M.; Flower, D.; Lopez, E.; Kyle, S.; Meuth, M.; Curtin, N. J.; Helleday, T. Specific killing of BRCA2-deficient tumours with inhibitors of poly(ADP-ribose) polymerase. *Nature* **2005**, *434*, 913–917.
- (16) Farmer, H.; McCabe, N.; Lord, C. J.; Tutt, A. N. J.; Johnson, D. A.; Richardson, T. B.; Santarosa, M.; Dillon, K. J.; Hickson, I.; Knights, C.; et al. Targeting the DNA repair defect in BRCA mutant cells as a therapeutic strategy. *Nature* **2005**, *434*, 917–921.
- (17) Lee, E. K.; Matulonis, U. A. PARP Inhibitor Resistance Mechanisms and Implications for Post-Progression Combination Therapies. *Cancers* **2020**, *12* (8), 2054.
- (18) Dias, M. P.; Moser, S. C.; Ganesan, S.; Jonkers, J. Understanding and overcoming resistance to PARP inhibitors in cancer therapy. *Nat. Rev. Clin. Oncol.* **2021**, *18*, 773–791.
- (19) Jiang, F.; Wang, H. J.; Jin, Y. H.; Zhang, Q.; Wang, Z. H.; Jia, J. M.; Liu, F.; Wang, L.; Bao, Q. C.; Li, D. D.; et al. Novel Tetrahydropyrido[4,3-*d*]pyrimidines as Potent Inhibitors of Chaperone Heat Shock Protein 90. *J. Med. Chem.* **2016**, *59* (23), 10498–10519.
- (20) Lin, S.; Zhang, X.; Yu, Z.; Huang, X.; Xu, J.; Liu, Y.; Wu, L. Synthesis of novel dual target inhibitors of PARP and EGFR and their antitumor activities in triple negative breast cancers. *Bioorg. Med. Chem.* **2022**, *61*, 116739.
- (21) You, Q. D.; Sun, H. P.; Jiang, F.; et al. Tetrahydropyrido [4,3-*d*] pyrimidine Hsp90 inhibitors and their medical uses. CN 105237533 B, 2017.
- (22) Vogel, C. L.; Cobleigh, M. A.; Tripathy, D.; Gutheil, J. C.; Harris, L. N.; Fehrenbacher, L.; Slamon, D. J.; Murphy, M.; Novotny, W. F.; Burchmore, M.; et al. Efficacy and Safety of Trastuzumab as a Single Agent in First-Line Treatment of HER2-Overexpressing Metastatic Breast Cancer. *J. Clin. Oncol.* **2002**, *20*, 719–726.
- (23) Pohlmann, P. R.; Mayer, I. A.; Mernaugh, R. Resistance to Trastuzumab in Breast Cancer. *Clin. Cancer Res.* **2009**, *15*, 7479–7491.
- (24) Bajrami, I.; Frankum, J. R.; Konde, A.; Miller, R. E.; Rehman, F. L.; Brough, R.; Campbell, J.; Sims, D.; Rafiq, R.; Hooper, S.; et al. Genome-wide Profiling of Genetic Synthetic Lethality Identifies CDK12 as a Novel Determinant of PARP1/2 Inhibitor Sensitivity. *Cancer Res.* **2014**, *74*, 287–297.
- (25) Genta, S.; Martorana, F.; Stathis, A.; Colombo, I. Targeting the DNA damage response: PARP inhibitors and new perspectives in the landscape of cancer treatment. *Crit. Rev. Oncol. Hematol.* **2021**, *168*, 103539.